Physiol Genomics 11: 21–30, 2002.
First published August 20, 2002; 10.1152/physiolgenomics.00062.2002.

Angiotensin II is associated with activation of NF-κB-mediated genes and downregulation of PPARs

DORIS M. THAM,[1] BABY MARTIN-MCNULTY,[3] YI-XIN WANG,[3] DENNIS W. WILSON,[2] RONALD VERGONA,[3] MARK E. SULLIVAN,[3] WILLIAM DOLE,[4] AND JOHN C. RUTLEDGE[1]
[1]*Department of Internal Medicine, School of Medicine, and* [2]*Department of Pathology, Microbiology and Immunology, School of Veterinary Medicine, University of California at Davis, Davis 95616; and* [3]*Departments of Pharmacology and* [4]*Cardiovascular Research, Berlex Biosciences, Richmond, California 94804*

Received 24 May 2002; accepted in final form 19 August 2002

Tham, Doris M., Baby Martin-McNulty, Yi-Xin Wang, Dennis W. Wilson, Ronald Vergona, Mark E. Sullivan, William Dole, and John C. Rutledge. Angiotensin II is associated with activation of NF-κB-mediated genes and downregulation of PPARs. *Physiol Genomics* 11: 21–30, 2002. First published August 20, 2002; 10.1152/physiolgenomics.00062.2002.—Angiotensin II (ANG II) promotes vascular inflammation through nuclear factor-κB (NF-κB)-mediated induction of pro-inflammatory genes. The role of peroxisome proliferator-activated receptors (PPARs) in modulating vascular inflammation and atherosclerosis in vivo is unclear. The aim of the present study was to examine the effects of ANG II on PPARs and NF-κB-dependent pro-inflammatory genes in the vascular wall in an in vivo model of atherosclerosis and aneurysm formation. Six-month-old male apolipoprotein E-deficient (apoE-KO) mice were treated with ANG II (1.44 mg/kg per day for 30 days). ANG II enhanced vascular inflammation, accelerated atherosclerosis, and induced formation of abdominal aortic aneurysms. These effects of ANG II in the aorta were associated with downregulation of both PPAR-α and PPAR-γ mRNA and protein and an increase in transcription of monocyte chemotactic protein-1 (MCP-1), macrophage-colony stimulating factor (M-CSF), endothelial-selectin (E-selectin), intercellular adhesion molecule-1 (ICAM-1), vascular cell adhesion molecule-1 (VCAM-1), inducible nitric oxide synthase (iNOS), and cyclooxygenase-2 (COX-2) throughout the entire aorta. ANG II also activated NF-κB with increases in both p52 and p65 NF-κB subunits. In summary, these in vivo results indicate that ANG II, through activation of NF-κB-mediated pro-inflammatory genes, promotes vascular inflammation, leading to acceleration of atherosclerosis and induction of aneurysm in apoE-KO mice. Downregulation of PPAR-α and -γ by ANG II may diminish the anti-inflammatory potential of PPARs, thus contributing to enhanced vascular inflammation.

aneurysm; atherosclerosis; chemokines; endothelial cell adhesion molecules

CHRONIC INFLAMMATION is a hallmark of atherosclerosis. The expression of chemokines, adhesion molecules, inducible nitric oxide synthase (iNOS), cyclooxygenase-2 (COX-2), and other genes associated with vascular injury and inflammation in atherosclerosis are mediated predominantly by nuclear factor-κB (NF-κB) (2, 7, 9, 13). Angiotensin II (ANG II), a potent vasoconstrictor, has been implicated in vascular inflammation and progression of atherosclerosis (4, 10, 17, 18, 38). It has been demonstrated that ANG II activates NF-κB (4, 32), which triggers the expression of pro-inflammatory and pro-oxidant genes implicated in the pathogenesis of atherosclerosis and its complications (1, 29, 30).

The peroxisome proliferator-activated receptors (PPARs) are members of the nuclear receptor superfamily of transcription factors that control the expression of a large array of genes. Experimental data indicate that both PPAR-α and -γ may play important roles in modulating vascular inflammation. Inflammation, induced by arachidonic acid or its derivative leukotriene B_4 (LTB_4), is prolonged in mice with targeted disruption of the PPAR-α gene (12). It has been suggested that many of these anti-inflammatory effects of PPARs may be due to inhibition of the NF-κB signaling pathway (11, 22, 36).

The present study examined the effects of ANG II on expression of a number of NF-κB-dependent pro-inflammatory genes and PPAR-α and -γ mRNA and protein expression in the vascular wall in an in vivo mouse model of atherosclerosis and aneurysm formation (10). Our data indicate that ANG II induces NF-κB-dependent pro-inflammatory genes and downregulates PPAR-α and -γ mRNA and protein expression in apoE-KO mice. Reduced PPAR expression may attenuate an important anti-inflammatory defense mechanism, thus contributing to ANG II-induced vascular inflammation.

METHODS

Animals. All animal protocols were approved by the Institutional Animal Care and Use Committee at the University of California at Davis and Berlex Biosciences. Osmotic minipumps (Alzet, model 2004; ALZA, Palo Alto, CA) containing either phosphate-buffered saline (PBS) or ANG II (1.44 $mg \cdot kg^{-1} \cdot day^{-1}$; Calbiochem, La Jolla, CA) were implanted subcutaneously in 6-mo-old male apolipoprotein E-deficient (apoE-KO) mice for 30 days. After 30 days, systolic

Article published online before print. See web site for date of publication (http://physiolgenomics.physiology.org).

Address for reprint requests and other correspondence: D. M. Tham, Dept. of Internal Medicine, One Shields Ave., TB 172, Davis, CA 95616 (E-mail: dmtham@ucdavis.edu).

blood pressure and heart rate were measured in conscious mice using a tail-cuff system (Kent Scientific, Litchfield, CT). Mice were trained to lie quietly in a restrainer placed on a warm pad for a period of at least 30 min for 1–4 days before the study. On the day of the study, the mice were placed in the temperature-controlled restrainer for 15 min. Blood pressure was then measured repeatedly and recorded on a data acquisition system (PowerLab, 16/s, ADInstruments, Australia). Systolic blood pressure and heart rate were averaged from five consecutive measurements. Mice were euthanized by CO_2 asphyxiation. The diameter of the suprarenal aorta was measured postmortem by direct measurement of cross sections.

Quantification of atherosclerosis. The left and right carotid arteries were dissected, cut open longitudinally, and pinned down individually on silicon-coated petri dishes. Atherosclerotic plaques were visible without staining. The images of the open luminal surface of both carotid arteries were recorded by a digital camera (Sony) mounted on a dissecting microscope. The plaque area was quantified using C-Imaging Systems (Compix, Cranberry Township, PA) and expressed as a percentage of the total luminal surface area of the carotid arteries.

Metabolic studies. Fasting serum levels of total cholesterol (TC), low-density lipoprotein (LDL), high-density lipoprotein (HDL), and triglyceride (TG) were measured by IDEXX (Sacramento, CA). Fasting serum glucose was measured on a Beckman glucose analyzer 2 (Beckman, Brea, CA) using the glucose oxidase method, and fasting insulin levels were assayed by radioimmunoassay (Linco Research, St. Charles, MI).

RT-PCR-based quantitative gene expression analysis. Real-time detection of PCR was performed using the GeneAmp 5700 sequence detection system (Applied Biosystems, Foster City, CA). The differential displays of aortic mRNAs for PPAR-α, PPAR-γ, monocyte chemotactic protein-1 (MCP-1), macrophage-colony stimulating factor (M-CSF), endothelial-selectin (E-selectin), intercellular adhesion molecule-1 (ICAM-1), vascular cell adhesion molecule-1 (VCAM-1), iNOS, and COX-2 were determined. Total RNA from four sections of the aorta (arch, thoracic, suprarenal, infrarenal) was isolated using an RNA isolation reagent (RNeasy kit; QIAGEN, Valencia, CA). Total RNA was used to generate cDNA for oligo-dT oligodeoxynucleotide primer ($_{T12-18}$) following the protocol for SuperScript II RNase H-reverse transcriptase (Life Technologies, Rockville, MD). The following primers were designed using Primer Express software (Applied Biosystems) and synthesized by Operon (Alameda, CA): PPAR-α, 5′-CCTCTTCCCAAAGCTCCTTCA-3′ (forward), 5′-CTGCGTCGGACTCGGTCTT-3′ (reverse); PPAR-γ, 5′-GAGATCATCTACACGATGCTGGC-3′ (forward), 5′-CGCAGGCTTTTGAGGAACTC-3′ (reverse); MCP-1, 5′-CAGCCAGATGCAGTTAACGC-3′ (forward), 5′-GCCTACTCATTGGGATCATCTTG-3′ (reverse); M-CSF, 5′-AGCATGGACAGGCAGGGAC-3′ (forward), 5′-CTGCGTGCCTTTATGCCTTT-3′ (reverse); E-selectin, 5′-GGCAGACATATTGGCTTTATCCC-3′ (forward), 5′-GATGGATCTCATGCTGGCTTC-3′ (reverse); ICAM-1, 5′-GAGTTTTACCAGCTATTTATTGAGTACCC-3′ (forward), 5′-CTCTCACAGCATCTGCAGCAG-3′ (reverse); VCAM-1, 5′-TTAAAGTCTGTGGATGGCTCGTAC-3′ (forward), 5′-CTTAATTGTCAGCCAACTTCAGTCTT-3′ (reverse); iNOS, 5′-GATGGTCCGCAAGAGAGTGC-3′(forward), 5′-AACGTAGACCTTGGGTTTGCC-3′(reverse); COX-2, 5′-TACAAGCAGTGGCAAAGGCC-3′(forward), 5′-TGATGTGTACGGCTTCAGGG-3′(reverse); GAPDH, 5′-GCAACAGGGTGGTGGACCT-3′ (forward), 5′-GGATAGGGCCTCTCTTGCTCA-3′ (reverse); vWF, 5′-AATGCCTTATTGGCGAGCAC-3′ (forward), 5′-CACTGCTTGCTGTACACCAGAAA-3′ (reverse).

Equal amounts of cDNA were used in duplicates and amplified with the SYBR Green I Master Mix (Applied Biosystems). The thermal cycling parameters were as follows: thermal activation for 10 min at 95°C, and 40 cycles of PCR (melting for 15 s at 95°C and annealing/extension for 1 min at 60°C). A standard curve was constructed with a dilution curve (1:5, 1:10, 1:20, 1:40, 1:80, 1:160, 1:320, 1:640) of total RNA from mouse aorta. A "no template control" was included with each PCR. Amplification efficiencies were validated and normalized against GAPDH or von Willebrand factor (vWF). Correct PCR product size was confirmed by electrophoresis through a 1% agarose gel stained with ethidium bromide. Purity of the amplified PCR products was determined by a heat-dissociation protocol.

ELISA. Serum soluble factors, sMCP-1 (Biosource International, Belgium) and sICAM-1 (Endogen, Woburn, MA), were measured by ELISA. Samples bound to gelatin that had been immobilized onto microtiter wells were detected with a monoclonal antibody raised against that particular mouse plasma soluble factor. The assay was developed with horseradish peroxidase (HRP) conjugate antibody against rabbit IgG and 3,3′,5,5′-tetramethylbenzidine (TMB) substrate, and the reaction was stopped with 2 mM H_2SO_4. Samples were appropriately diluted for each assay.

Western blot analysis. Whole aortas were collected and rinsed in PBS for analysis of protein expression. Cytoplasmic and nuclear extracts of aortic tissue were isolated using NE-PER Nuclear and Cytoplasmic Extraction Reagents (Pierce, Rockford, IL) and a protease inhibitor cocktail (Sigma Chemical, St. Louis, MO). Tissues were homogenized on ice using a Tissue Tearor (Biospecs Products, Racine, WI). Protein concentration was measured by a modified Lowry assay kit (Bio-Rad, Hercules, CA), using bovine IgG as the standard. Fifty micrograms of cytoplasmic tissue extract and 10 μg of nuclear tissue extract were electrophoresed on 12.5% SDS-polyacrylamide gels under reducing conditions (100 mM DTT) and transferred onto a membrane (Immobilon-P PVDF; Millipore, Woburn, MA) using a semi-dry electroblotter (Owl Scientific, Woburn, MA). The membranes were blocked with Tris-buffered saline (TBS) containing 0.05% polyethylene-sorbitan monolaurate (Tween 20) (TBST) and 10% (wt/vol) nonfat dry milk at room temperature for 1 h and then incubated for 1 h with the primary antibody. The primary antibodies were as follows: 5 μg/ml dilution of PPAR-α (goat polyclonal antibodies raised against a peptide corresponding to amino acids 2–21 mapped at the amino terminus of the human PPAR-α) (Research Diagnostics, Flanders, NJ) and 1:100 dilution of PPAR-γ (rabbit polyclonal antibodies raised against a recombinant protein corresponding to amino acids 6–105 sequence mapping to the amino terminus of PPAR-γ of human origin) (Santa Cruz Biotechnology, Santa Cruz, CA). After washing the membranes in TBST, the immunoblots were incubated with the secondary antibody goat anti-rabbit IgG-HRP (Santa Cruz Biotechnology) for PPAR-α and donkey anti-rabbit IgG-HRP (Pierce) for PPAR-γ at a 1:15,000 dilution for 1 h at room temperature. The blots were then developed with Super Signal West Pico Chemiluminescent Substrate (Pierce). Blots were exposed to X-ray film and were quantified using the Kodak Electrophoresis Documentation and Analysis System 290 (Eastman-Kodak, Rochester, NY). Blots were stripped with Restore Western blot stripping buffer (Pierce) and reprobed with a 1:15,000 dilution of smooth muscle actin (Research Diagnostics) and secondary anti-mouse antibody at a 1:15,000 dilution (Santa Cruz Bio-

technology) as a loading control. Both cytoplasmic PPAR-α and -γ were normalized to actin.

Immunohistochemistry. At the end of each experiment, the aorta was perfused at a constant pressure of 100 mmHg through the heart with PBS followed by warm (37°C) agarose (Sea-Plaque GTG Agarose, low melt; FRMC BioProducts, Rockland, ME) diluted in saline (3% wt/vol) and colored with a green tissue dye. After the agarose had solidified, the abdominal aorta was dissected free from the surrounding connective tissue and pinned onto a wax block before fixation in 10% formalin. Cross sections of aorta (2.5 mm in thickness) were made between the superior mesenteric and right renal arteries. A small portion of the right renal artery was left attached to the samples to facilitate orientation of the specimen. These tissues were dehydrated through a graded ethanol series, cleared with xylene, infiltrated with warm paraffin, embedded in paraffin blocks, and cut at 5-μm thick sections onto gelatin-coated glass slides. The sections were first treated with 0.3% H_2O_2 in PBS for 30 min to abolish endogenous peroxidase activity. Sections then were incubated for 1 h at room temperature with the following primary antibodies: 10 μg/ml dilution of PPAR-α (goat polyclonal antibodies raised against a peptide corresponding to amino acids 2–21 mapped at the amino terminus of the human PPAR-α) (Research Diagnostics) and 1:200 dilution PPAR-γ (rabbit polyclonal antibodies raised against a peptide corresponding to amino acids 82–101 of human PPAR-γ) (Cayman Chemical, Ann Arbor, MI). After several washes with PBS, sections were detected with streptavidin-HRP at a 1:100 dilution plus nickel-enhanced 3,3′-diaminobenzidine (DAB) and counterstained with hematoxylin. Rabbit IgG was used as a negative control (Sigma Chemical). Parallel staining using anti-macrophage antibody (Mac-3; BD Pharmingen, San Diego, CA) and anti-smooth muscle actin antibody confirmed that PPAR-α- and PPAR-γ-positive cells were macrophages and smooth muscle cells, respectively. Separate sections were stained with hematoxylin and eosin.

Assessment of NF-κB activation by electrophoretic mobility shift assay (EMSA). Nuclear extracts of aortic tissue were isolated using NE-PER Nuclear and Cytoplasmic Extraction Reagents (Pierce). Protein concentrations were determined as described above. The NF-κB consensus oligonucleotide (5′-AGTTGAGGGGACTTTCCCAGGC-3′; Santa Cruz Biotechnology) was 3′ end-labeled with biotin (Pierce). The binding reactions containing equal amounts of protein (10 μg) and 20 fmol of oligonucleotide were performed for 20 min in binding buffer [2.5% glycerol, 5 mmol/l $MgCl_2$, 50 ng/μl poly(dI-dC), 0.05% NP-40; Pierce]. The reaction volumes were held constant to 20 μl. For supershift assays, 1 μl of polyclonal antibody to NF-κB1 (p50), NF-κB2 (p52), or Rel A (p65) (Santa Cruz Biotechnology) was added to the binding reactions. The reaction products were separated in a 6% polyacrylamide gel, detected with streptavidin-HRP and analyzed by autoradiography. For detection of nuclear NF-κB subunits, polyclonal antibody to p50, p52, or p65 was used at a 1:100 dilution in a Western blot analysis as previously described. The NF-κB activation was quantified using the Kodak Electrophoresis Documentation and Analysis System 290 (Eastman-Kodak). For competition assays, 50 ng of unlabeled oligonucleotide was added to the nuclear extracts before formulation of DNA/protein complexes to confirm the specificity of this NF-κB binding assay. A mutant NF-κB consensus oligonucleotide (Santa Cruz Biotechnology) was used as a negative control.

Statistical analysis. Data are means ± SE. Statistical analysis was performed between two groups using two-tailed Student's *t*-test for unpaired values, one-way ANOVA (with a Bonferroni post hoc test) for normally distributed populations, and Kruskal-Wallis ANOVA (with a Dunn's post hoc test) for nonnormally distributed populations, when comparing groups of three or more. $P < 0.05$ was considered statistically significant.

Table 1. *Effects of angiotensin II in apolipoprotein E-deficient mice*

	Vehicle	ANG II
Body wt, g	29.3 ± 0.6 (16)	27.5 ± 0.3† (20)
Systolic blood pressure, mmHg	124 ± 4 (4)	160 ± 12* (7)
Carotid plaque area, %	5 ± 1.9 (4)	34.6 ± 3.6‡ (10)
Diameter of suprarenal aorta, mm	0.89 ± 0.02 (7)	1.9 ± 0.2‡ (12)
Total cholesterol, mg/dl	589 ± 35 (26)	637 ± 28 (24)
LDL, mg/dl	552 ± 42 (18)	523 ± 21 (25)
HDL, mg/dl	43 ± 3 (19)	65 ± 5‡ (25)
Triglyceride, mg/dl	172 ± 11 (20)	237 ± 21† (25)
Glucose, mg/dl	115 ± 9 (26)	107 ± 7 (24)
Insulin, ng/dl	0.58 ± 0.06 (14)	0.54 ± 0.05 (13)

Data are means ± SE; no. of animals is in parentheses. *$P < 0.05$, †$P < 0.01$, and ‡$P < 0.001$, significantly different from vehicle.

RESULTS

Chronic infusion (30 days) of ANG II in apoE-KO mice resulted in an increase in systolic blood pressure and a sixfold increase in carotid plaque area (Table 1). All mice treated with ANG II developed aneurysms that were consistently localized to the suprarenal region of the abdominal aorta. None of the vehicle-treated mice developed aneurysms. The average outer diameter of the suprarenal aorta of the ANG II-treated group was approximately twofold greater than that of the vehicle controls ($P < 0.001$). Compared with the vehicle controls, the ANG II-treated mice showed a slight decrease in body weight, a 38% increase in serum TG, and a 51% increase in HDL, with no significant effects on TC, LDL, or fasting serum glucose and insulin levels.

ANG II decreased expression of PPAR-α and PPAR-γ in the aortic wall. ANG II treatment was associated with a reduction of the mRNA levels of both PPAR-α and PPAR-γ in all four sections of the aorta (arch, thoracic, suprarenal, infrarenal) compared with the vehicle controls (Fig. 1). Specifically, ANG II treatment significantly decreased PPAR-α gene expression in the arch, suprarenal, and infrarenal aorta compared with vehicle controls. ANG II treatment reduced PPAR-γ gene expression by 45–85% throughout the entire aortic tree, although this was not statistically significant. PPAR gene expression was not statistically significant between the four sections of the aorta within each treatment group. Western blot analysis of the aorta detected PPAR-α and -γ protein in both the cytoplasmic and nuclear protein fractions. The expression of both cytoplasmic and nuclear PPAR-α protein was significantly decreased by 46% ($P < 0.05$) and 8% ($P < 0.001$), respectively, in the ANG II-treated group compared with the vehicle controls (data not shown). The expression of both cytoplasmic and nuclear PPAR-γ

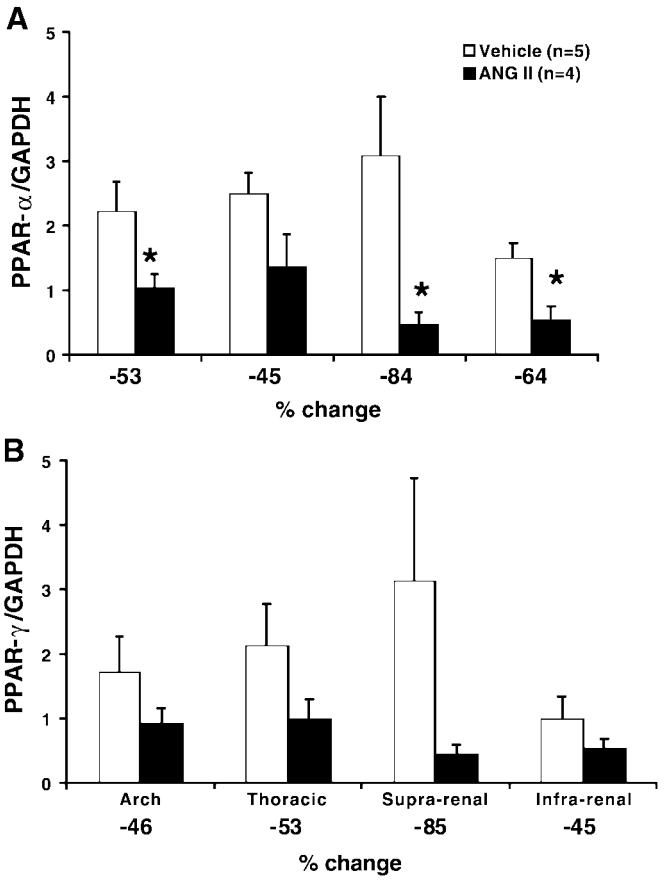

Fig. 1. Expression of peroxisome proliferator-activated receptor-α (PPAR-α , *A*) and PPAR-γ (*B*) mRNA in the aortas of apolipoprotein E-deficient (apoE-KO) mice treated with ANG II or vehicle. Total RNA extracted from individual aortic sections (arch, thoracic, suprarenal, infrarenal) was subjected to quantitative RT-PCR using primers specific for PPAR-α and -γ. Values were normalized to GAPDH and are means ± SE. $*P < 0.05$, significantly different from vehicle.

protein was decreased by 136% ($P < 0.05$) and 41% ($P = 0.066$), respectively, in the ANG II-treated group compared with the vehicle controls (Fig. 2). Compared with the vehicle group, histological examination showed that the aortas from ANG II-treated mice (Fig. 3, *A* and *B*) had thickened media and increased cellularity evident in the adventitia due to increased numbers of mononuclear cells. Morphologically, these monocytes appeared to be macrophages and were identified with positive Mac-3 staining (data not shown). The aortic intimal plaques in the ANG II group contained polygonal cells with vesicular cytoplasm (Fig. 3, *D* and *F*). The luminal surface of the plaques was lined by endothelium. Immunohistochemistry detected PPAR-α protein lightly stained the endothelium, elastin fibers, and foci in smooth muscle cytoplasm of both vehicle (Fig. 3*C*) and ANG II-treated (Fig. 3*D*) mice. Intimal plaques in ANG II-treated mice did not stain for PPAR-α (Fig. 3*D*), but PPAR-γ was strongly expressed in the neointima (Fig. 3*F*). PPAR-γ stained strongly positive in the endothelium of the aorta from the ANG II group, but was diffusely positive compared with vehicle controls (Fig. 3, *E* and *F*). A significant PPAR-γ signal was also present in the extracellular matrix of the adventitia of both groups (Fig. 3, *E* and *F*). Medial smooth muscle cells of the aorta from the ANG II-treated mice showed focal perinuclear PPAR-γ staining, and there was lightly positive and diminished (relative to vehicle) PPAR-γ staining of extracellular matrix in the adventitia (Fig. 3, *E* and *F*). All sections incubated with rabbit IgG antibody were negative (data not shown).

ANG II increased expression of pro-inflammatory genes. The mRNA levels of the chemokines (MCP-1 and M-CSF) (Fig. 4), the endothelial cell adhesion molecules (E-selectin, ICAM-1, VCAM-1) (Fig. 5), and iNOS and COX-2 (Fig. 6) were increased in all four sections of aortas from the ANG II-treated group compared with the vehicle group. Specifically, ANG II treatment increased MCP-1 gene expression by 208–494% (with statistical significance in the suprarenal aorta) and M-CSF gene expression by 40–515% (with statistical significance in the arch and suprarenal aorta) (Fig. 4). In the ANG II-treated aortas, E-selectin gene expression was increased by 20–106% (with statistical signif-

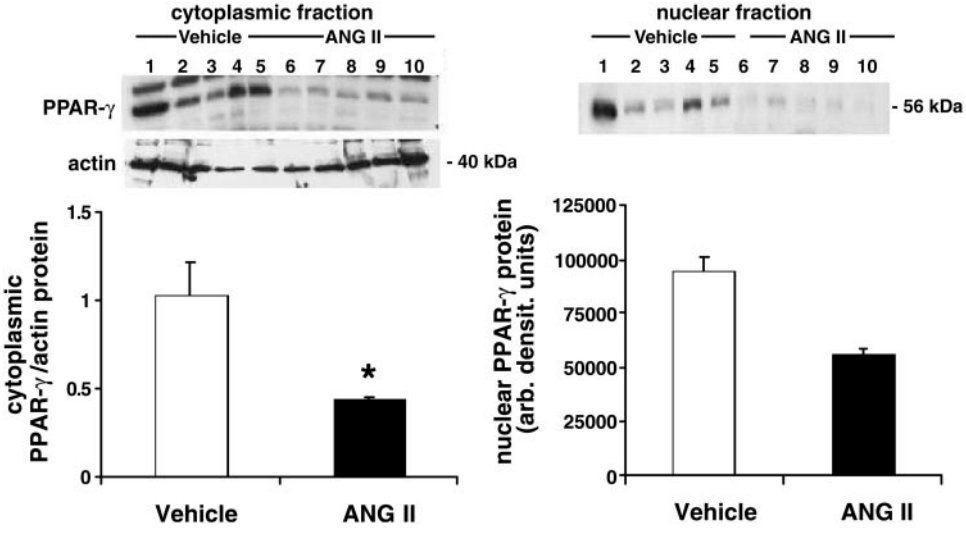

Fig. 2. Expression of PPAR-γ protein in the aorta of apoE-KO mice treated with ANG II or vehicle. Western blot analysis detected PPAR-γ protein (56 kDa) in the cytoplasmic (*left*) and nuclear (*right*) compartments. Protein bands were quantified by densitometry. Cytoplasmic protein levels were normalized to actin (40 kDa). Nuclear protein levels were expressed as arbitrary densitometry units. Values are means ± SE. $*P < 0.05$, significantly different from vehicle.

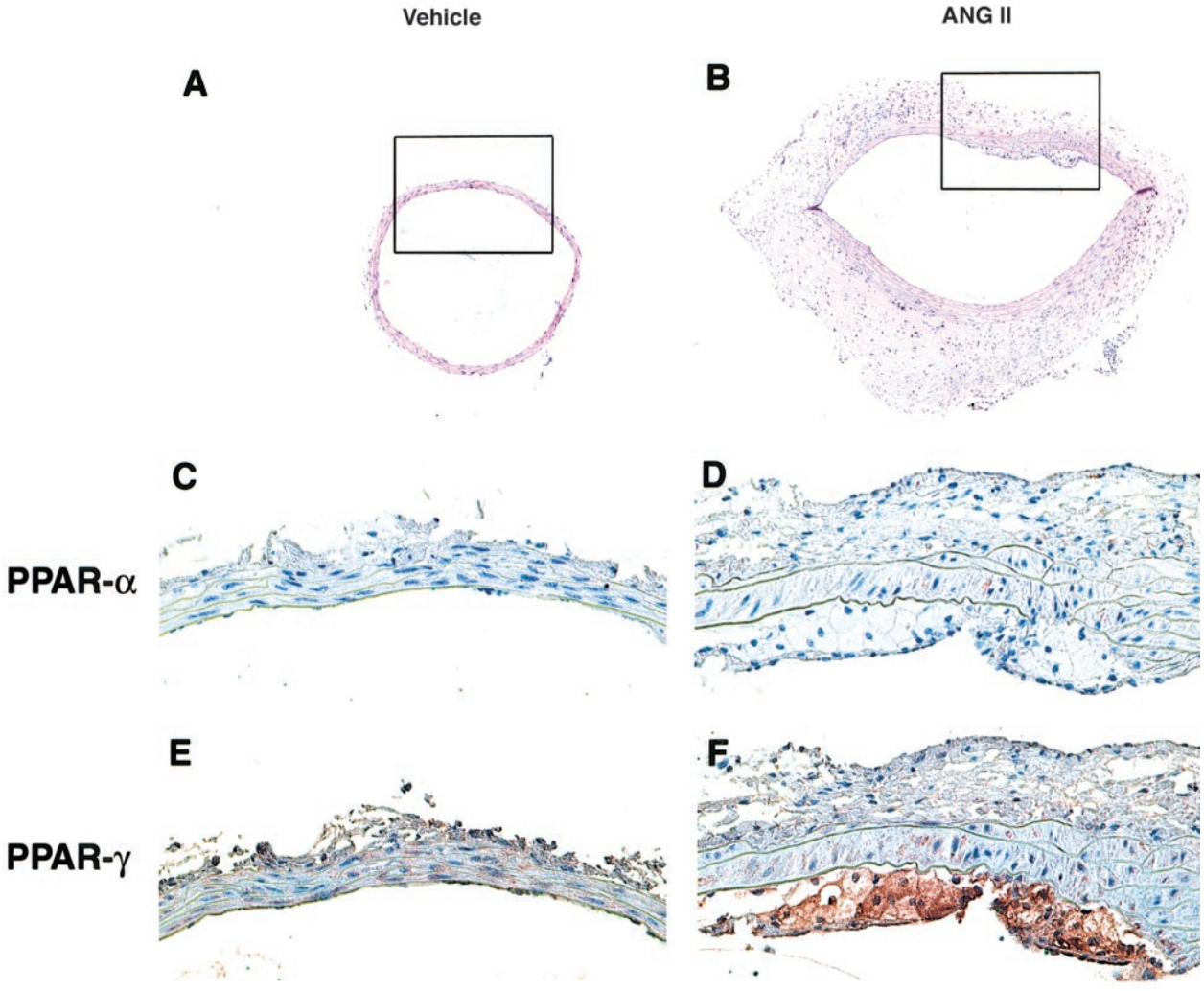

Fig. 3. Histological and immunohistochemical appearance of the suprarenal aorta from apoE-KO mice treated with ANG II (*right*) or vehicle (*left*). Hematoxylin and eosin staining of vehicle (*A*) and ANG II-treated aorta (*B*). In the ANG II-treated aorta, both the media and adventitia are expanded by extracellular matrix with increased cellularity in the adventitia. Vehicle and ANG II-treated aortas were lightly positive for PPAR-α staining in the endothelial and smooth muscle cells (*C* and *D*). The intimal plaques of polygonal vesicular cells in ANG II-treated aortas were negative for PPAR-α (*D*). Vehicle and ANG II-treated aortas demonstrated evident staining with PPAR-γ on endothelial and focal smooth muscle cells (*E* and *F*). Aortas from ANG II treatments demonstrated positive PPAR-γ staining in the intimal plaques that are overlain by positive staining endothelial cells (*F*). Original magnifications: ×11 (*A* and *B*), ×2,150 (*C–F*).

icance in the thoracic and suprarenal aorta), ICAM-1 gene expression was increased by 68–239%, and VCAM-1 gene expression was increased by 409–958% (with statistical significance in the thoracic, suprarenal, and infrarenal aorta) (Fig. 5). Although no statistical significance was observed, ANG II treatment increased aortic gene expression of iNOS by 14–29% and COX-2 by 43–382% (Fig. 6). The expression of these pro-inflammatory genes was not statistically significant between the four sections of the aorta within each treatment group. Despite increases in transcription of MCP-1 and ICAM-1 in the aorta, there were no significant differences detected in serum soluble MCP-1 (134 ± 11 vs. 145 ± 5 ng/ml) or soluble ICAM-1 (43 ± 5 vs. 33 ± 3 ng/ml) between the vehicle and ANG II groups (n = 12–15/group), respectively.

ANG II activated the NF-κB pathway. Compared with the vehicle controls, nuclear extracts from the aortas of the ANG II group displayed a 53% increase ($P < 0.05$) in the activation of NF-κB, and competition assays with unlabeled NF-κB oligonucleotides confirmed the specificity of this NF-κB DNA binding assay (EMSA, Fig. 7, *A* and *B*). In this particular phase of NF-κB binding, Western blot analysis detected a 29% increase in the p52 subunit ($P < 0.05$, Fig. 7*C*) and a 20% increase in the p65 subunit ($P = 0.06$, Fig. 7*D*) in the aortas of the ANG II group compared with those of the vehicle group. Supershift assays with the p52 and P65 subunit confirmed the specificity of this NF-κB DNA binding assay (data not shown). The p50 subunit was not detected in the nuclear extracts in either treatment groups (data not shown). As expected, reac-

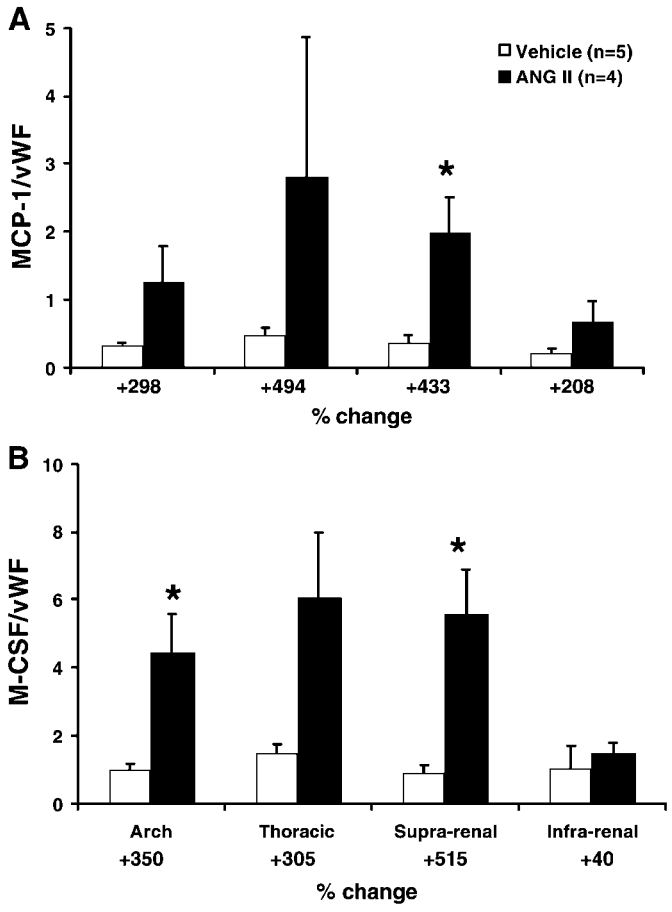

Fig. 4. Expression of monocyte chemotactic protein-1 (MCP-1, *A*) and macrophage-colony stimulating factor (M-CSF, *B*) mRNA in the aortas of apoE-KO mice treated with ANG II or vehicle. Total RNA extracted from individual aortic sections (arch, thoracic, suprarenal, infrarenal) was subjected to quantitative RT-PCR using primers specific for MCP-1 and M-CSF. Values were normalized to von Willebrand factor (vWF) and are means ± SE. $*P < 0.05$, significantly different from vehicle.

tions with the NF-κB mutant oligonucleotide resulted in no detectable activation.

DISCUSSION

In the present study, administration of ANG II for 30 days to apoE-KO mice markedly enhanced vascular inflammation, the development of atherosclerosis, and aneurysm formation. These changes were associated with an increase in mononuclear cell infiltrations in the aortic wall and mRNA expression of a number of pro-inflammatory mediators including: chemokines (MCP-1, M-CSF) and endothelial cell adhesion molecules (E-selectin, VCAM-1). Concomitant with the enhanced pro-inflammatory response, ANG II treatment also decreased expression of both PPAR-α and PPAR-γ mRNA and protein in the aortic wall.

There is in vivo evidence to indicate that PPARs can modulate the development and severity of atherosclerosis. Li et al. (20) reported that administration of the PPAR-γ activator, rosiglitazone or GW-7845, reduced the extent of atherosclerosis in LDL receptor-deficient (LDLR-KO) mice. PPAR-α-deficient mice had a prolonged inflammatory response (12), and transplantation of PPAR-γ-null bone marrow into LDLR-KO mice resulted in a significant increase in atherosclerosis (6).

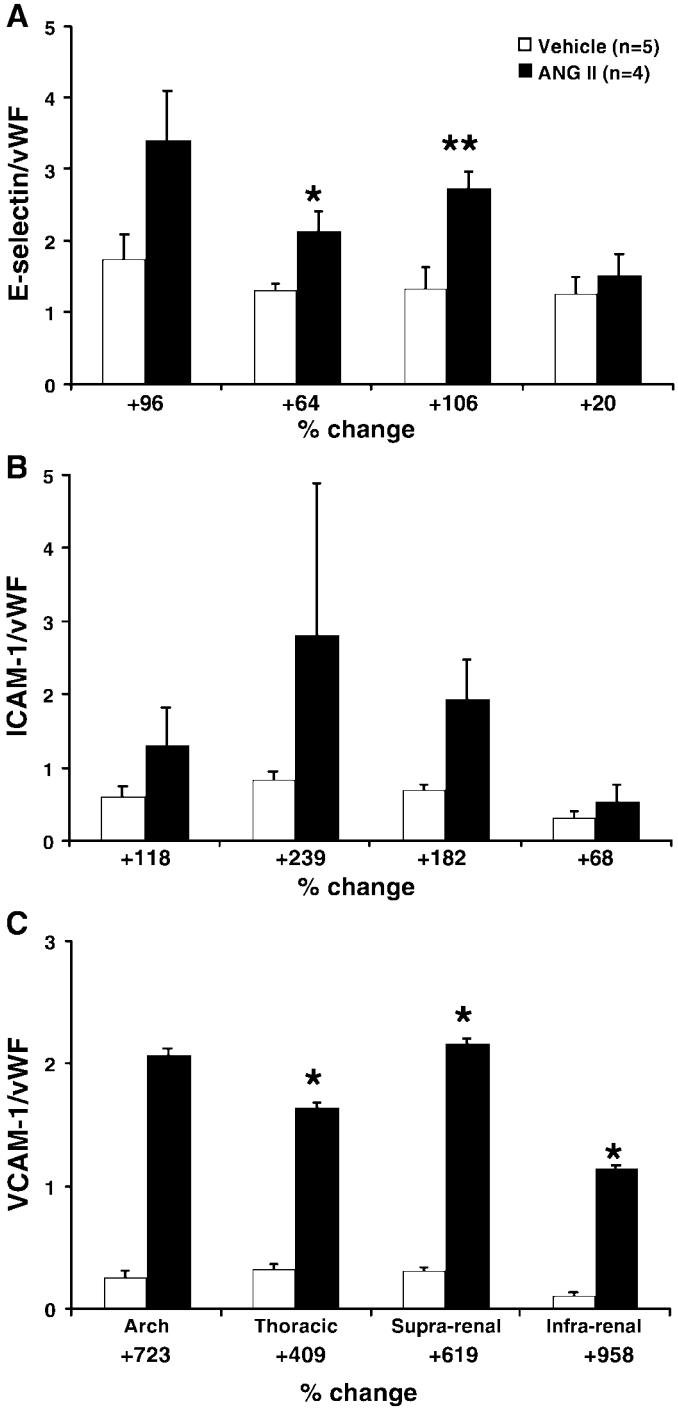

Fig. 5. Expression of endothelial-selectin (E-selectin, *A*), intercellular adhesion molecule-1 (ICAM-1, *B*), and vascular cell adhesion molecule-1 (VCAM-1, *C*) mRNA in the aortas of apoE-KO mice treated with ANG II or vehicle. Total RNA extracted from individual aortic sections (arch, thoracic, suprarenal, infrarenal) was subjected to quantitative RT-PCR using primers specific for E-selectin, ICAM-1, and VCAM-1. Values were normalized to vWF and are means ± SE. $*P < 0.05$ and $**P < 0.01$, significantly different from vehicle.

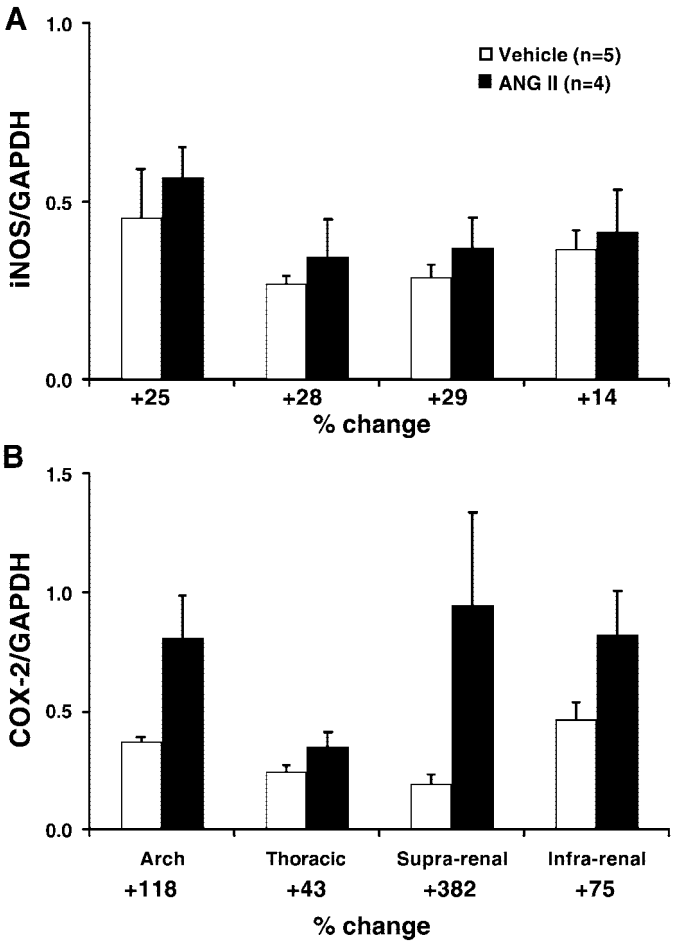

Fig. 6. Expression of inducible nitric oxide synthase (iNOS, *A*) and cyclooxygenase-2 (COX-2, *B*) mRNA in the aortas of apoE-KO mice treated with ANG II or vehicle. Total RNA extracted from individual aortic sections (arch, thoracic, suprarenal, infrarenal) was subjected to quantitative RT-PCR using primers specific for iNOS and COX-2. Values were normalized to GAPDH and are means ± SE.

These reports are consistent with an anti-inflammatory and anti-atherosclerotic role for PPARs. Based on such a role, the concomitant downregulation of PPAR-α and -γ by ANG II in the present study would be expected to contribute to the observed enhanced vascular inflammation and accelerated atherosclerosis in apoE-KO mice, probably due to the compromised anti-inflammatory potential of PPARs.

The NF-κB transcription factor has a major role in regulating pro-inflammatory genes implicated in the progression of atherosclerosis. These include adhesion molecules, cytokines, chemokines, interferons, growth factors, and other mediators, such as iNOS and COX-2 (19, 21, 25, 26, 34). There is differential induction of NF-κB complexes during the time course of NF-κB activation. NF-κB is composed of the transactivator subunits, Rel A (p65) and c-rel, and the DNA binding subunits, NF-κB1 (p50) and NF-κB2 (p52), which form various hetero- and homodimers (35). In unstimulated cells, NF-κB subunits are associated with the inhibitory protein, IκB, resulting in inactivation of DNA binding activity by preventing translocation of NF-κB into the nucleus. Once activated, NF-κB binds to recognition elements in the promoter region of pro-inflammatory genes and acts as a dominant regulator of transcription of these genes to induce inflammation (3). Since activation of NF-κB is linked to enhanced expression of genes predominantly implicated in atherogenesis, we examined whether ANG II treatment was also associated with increased NF-κB activation, thus leading to vascular inflammation. Indeed, EMSA showed that aortic NF-κB nuclear translocation was significantly enhanced, and Western blot analysis of nuclear aortic extracts demonstrated that the NF-κB subunits (p52 and p65) were increased following ANG II treatment compared with vehicle controls. These data suggest that Rel A:NF-κB2 nuclear translocation following ANG II treatment may be responsible for the activation of NF-κB, which in turn, mediates NF-κB-dependent expression of chemokines, endothelial cell adhesion molecules, iNOS, and COX-2. Previous studies have also demonstrated that ANG II induces interleukin-6 (IL-6) transcription through the pleiotropic activation of NF-κB (16). In our earlier study, ANG II increased secretion of IL-6 protein from the aneurysmal segment by 2.4-fold compared with vehicle treatment (37). The overexpression of these pro-inflammatory mediators in the vascular wall observed in the present study may have disrupted homeostatic anti-inflammatory mechanisms, thus leading to atherogenesis and aneurysm formation.

Other studies have demonstrated PPARs ability to interfere with the NF-κB signaling pathway (36). Some of these mechanisms include protein-protein interactions whereby NF-κB proteins are prevented from binding to their target sequences (22). For example, the natural PPAR-γ ligand, prostaglandin 15-deoxy-δ-12,14-prostaglandin J_2 (15-PDJ_2) was found to directly inhibit the IκB kinase which phosphorylates and inactivates IκB (31). In this study, we observed decreases in both PPAR-α and -γ mRNA and protein expression following ANG II treatment. We speculate that this decrease in PPAR expression by ANG II treatment may have diminished its inhibitory effect on the NF-κB signaling transduction pathway, thus inducing expression of NF-κB-dependent genes in the aorta, which contributed to the progress of atherosclerosis. Immunohistochemistry of the suprarenal aneurysmal segment from the ANG II-treated mice demonstrated localization of PPAR-α and -γ protein to endothelial cells, smooth muscle cells, and monocytic cells, indicating that PPARs may play a role in the pathogenesis of atherosclerosis, including modulation of endothelial activation, smooth muscle proliferation, and monocyte infiltration. Decreased PPAR-γ staining in the adventitia correlated with reduced mRNA and protein expression following ANG II treatment. As evident from our results, PPAR-γ protein was localized to both macrophages and foams cells in the neointima of ANG II-treated vessels, the most activated cells in atheroma. The role of PPAR-γ protein in the neointima of ANG II-treated vessels is unclear, but recently, it has been observed that PPAR-α or -γ activators induce

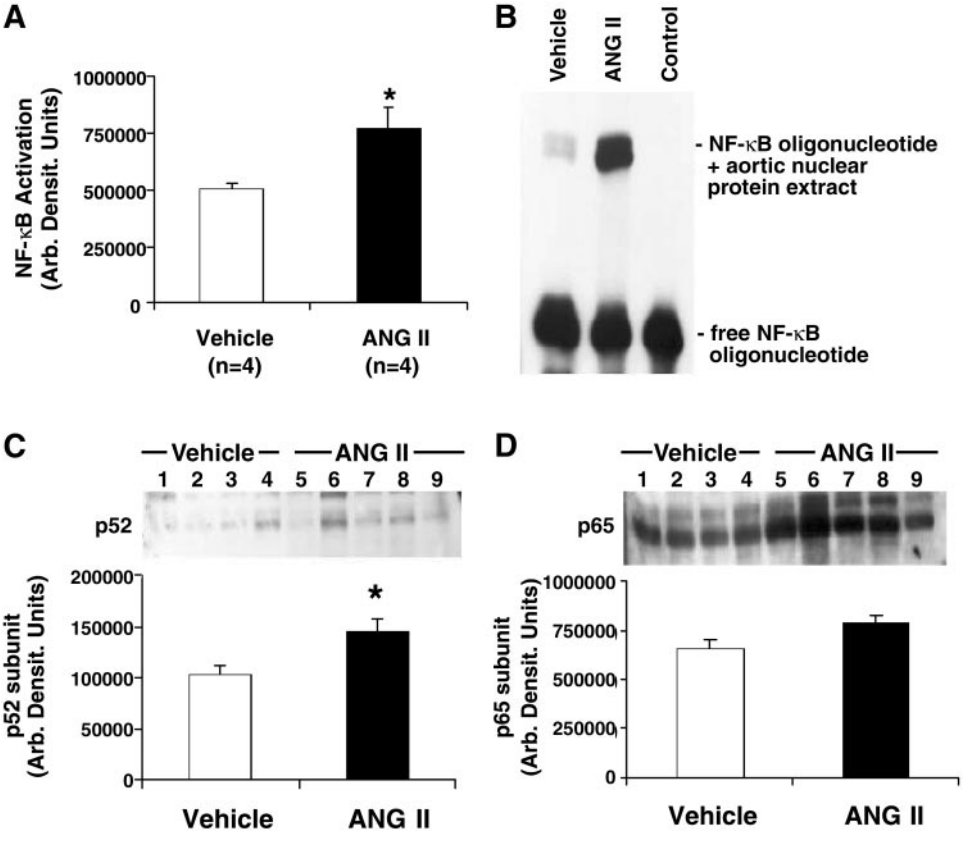

Fig. 7. Induction of nuclear factor-κB (NF-κB) binding activity in the aortas of apoE-KO mice treated with ANG II or vehicle. Nuclear extracts prepared from the aortas of apoE-KO mice were used to bind the 3′-biotin-labeled NF-κB oligonucleotide, and the appearance of the sequence-specific NF-κB binding activity was detected by electrophoretic mobility shift assay (EMSA) (*A* and *B*). Specificity of this NF-κB binding assay was determined by addition of 50 ng unlabeled NF-κB oligonucleotide (control) (*B*). Western blot analysis was performed on aortic nuclear extracts from apoE-KO mice using antibodies against the p52 and p65 NF-κB subunits (*C* and *D*). NF-κB activation and NF-κB subunit protein levels were quantified by densitometry and are expressed as arbitrary densitometry units. Values are means ± SE. $*P < 0.05$, significantly different from vehicle. Similar EMSA results were seen in 4 independent experiments.

cholesterol removal from human macrophage foam cells, indicating that PPAR agonists may counter the progression of atherosclerosis (8, 23). However, PPAR-γ activation has also been suggested to be involved in the differentiation of monocytes into macrophages (24, 27) and the promotion of foam cell formation through the transcriptional induction of CD36 in human macrophages leading to enhanced oxidized LDL uptake (24). Currently, it is still unclear whether activation of PPAR-α and -γ in macrophages promotes or inhibits atherogenesis. Further studies are warranted to determine the biological roles of PPARs in the macrophages/monocytes and foams cells and their effects on atherosclerosis.

In this study, ANG II treatment resulted in a significant increase in both systolic blood pressure and TG levels. Published studies have suggested that an increase in systolic blood pressure elicits an inflammatory response (14). Reports have also suggested a significant correlation between TGs and cellular mediators of inflammation (28). Therefore, we cannot rule out the possibility that the vascular inflammation observed in this study, in response to ANG II treatment, may be attributed to other factors such as increases in systolic blood pressure and/or TG levels.

We demonstrated in our previous study that vascular inflammation induced by ANG II in apoE-KO mice promoted the recruitment and infiltration of macrophages into the vascular wall and activated macrophage-derived urokinase-type plasminogen activator (uPA) in the aneurysmal segment (37). Activated uPA hydrolyzes plasminogen to form plasmin, which then activates an array of matrix metalloproteinase (MMPs). Both plasmin and activated MMPs degrade fibrin and elastin fibers, which are major components of the arterial extracellular matrix. Thus activation of the uPA-plasmin-MMP system enhances proteolysis of extracellular matrix and contributes to aneurysm formation. This is consistent with the report that uPA plays a key role in aneurysm formation in apoE-KO mice fed with high-cholesterol diet (5). In this study, however, we did not observe a significant difference in pro-inflammatory or PPAR gene expression between nonaneurysmal (arch, thoracic, and infrarenal aorta) and aneurysmal (suprarenal aorta) tissue in the ANG II-treated animals. Inflammatory infiltrate is the constant histological finding in the abdominal aortic aneurysmal wall (15, 33). The nature of chemotactic factors, which start the influx of inflammatory cells to the aortic wall, is unknown. Additional studies are needed to determine whether the specific expression of other pro-inflammatory genes in the suprarenal aorta may be specifically involved in ANG II-induced aneurysm formation.

In summary, the pro-inflammatory actions of ANG II in the vascular wall have been confirmed in vivo in this study. Downregulation of PPARs by ANG II may impair an important anti-inflammatory defense mechanism, thus contributing to the enhanced inflammatory response to ANG II in the artery wall.

We are grateful to Jefferson Davis for excellent technical assistance.

This work was supported by grants from the Biotechnology Strategic Targets for Alliances in Research, the Richard A. and Nora Eccles Harrison Endowed Chair in Diabetes Research, the American Federation for Aging Research, and National Heart, Lung, and Blood Institute Grant HL-55667.

REFERENCES

1. **Alexander RW.** Theodore Cooper Memorial Lecture. Hypertension and the pathogenesis of atherosclerosis Oxidative stress and the mediation of arterial inflammatory response: a new perspective. *Hypertension* 25: 155–161, 1995.
2. **Baeuerle PA and Henkel T.** Function and activation of NF-κB in the immune system. *Annu Rev Immunol* 12: 141–179, 1994.
3. **Barnes PJ.** Nuclear factor-κB. *Int J Biochem Cell Biol* 29: 867–870, 1997.
4. **Brasier AR, Jamaluddin M, Han Y, Patterson C, and Runge MS.** Angiotensin II induces gene transcription through cell-type-dependent effects on the nuclear factor-κB (NF-κB) transcription factor. *Mol Cell Biochem* 212: 155–169, 2000.
5. **Carmeliet P, Moons L, Lijnen R, Baes M, Lemaitre V, Tipping P, Drew A, Eeckhout Y, Shapiro S, Lupu F, and Collen D.** Urokinase-generated plasmin activates matrix metalloproteinases during aneurysm formation. *Nat Genet* 17: 439–444, 1997.
6. **Chawla A, Boisvert WA, Lee CH, Laffitte BA, Barak Y, Joseph SB, Liao D, Nagy L, Edwards PA, Curtiss LK, Evans RM, and Tontonoz P.** A PPARγ-LXR-ABCA1 pathway in macrophages is involved in cholesterol efflux and atherogenesis. *Mol Cell* 7: 161–171, 2001.
7. **Chen BC and Lin WW.** Pyrimidinoceptor potentiation of macrophage PGE(2) release involved in the induction of nitric oxide synthase. *Br J Pharmacol* 130: 777–786, 2000.
8. **Chinetti G, Lestavel S, Bocher V, Remaley AT, Neve B, Torra IP, Teissier E, Minnich A, Jaye M, Duverger N, Brewer HB, Fruchart JC, Clavey V, and Staels B.** PPAR-α and PPAR-γ activators induce cholesterol removal from human macrophage foam cells through stimulation of the ABCA1 pathway. *Nat Med* 7: 53–58, 2001. [comment in Nat Med 7: 23–24, 2001; UI 21065276].
9. **Collins T, Read MA, Neish AS, Whitley MZ, Thanos D, and Maniatis T.** Transcriptional regulation of endothelial cell adhesion molecules: NF-κB and cytokine-inducible enhancers. *FASEB J* 9: 899–909, 1995.
10. **Daugherty A, Manning MW, and Cassis LA.** Angiotensin II promotes atherosclerotic lesions and aneurysms in apolipoprotein E-deficient mice. *J Clin Invest* 105: 1605–1612, 2000.
11. **Delerive P, De Bosscher K, Besnard S, Vanden Berghe W, Peters JM, Gonzalez FJ, Fruchart JC, Tedgui A, Haegeman G, and Staels B.** Peroxisome proliferator-activated receptor α negatively regulates the vascular inflammatory gene response by negative cross-talk with transcription factors NF-κB and AP-1. *J Biol Chem* 274: 32048–32054, 1999.
12. **Devchand PR, Keller H, Peters JM, Vazquez M, Gonzalez FJ, and Wahli W.** The PPARα-leukotriene B4 pathway to inflammation control (see comments). *Nature* 384: 39–43, 1996.
13. **Du X, Stocklauser-Farber K, and Rosen P.** Generation of reactive oxygen intermediates, activation of NF-κB, and induction of apoptosis in human endothelial cells by glucose: role of nitric oxide synthase? *Free Radic Biol Med* 27: 752–763, 1999.
14. **Haller H, Park JK, Dragun D, Lippoldt A, and Luft FC.** Leukocyte infiltration and ICAM-1 expression in two-kidney one-clip hypertension. *Nephrol Dial Transplant* 12: 899–903, 1997.
15. **Halpern VJ, Nackman GB, Gandhi RH, Irizarry E, Scholes JV, Ramey WG, and Tilson MD.** The elastase infusion model of experimental aortic aneurysms: synchrony of induction of endogenous proteinases with matrix destruction and inflammatory cell response. *J Vasc Surg* 20: 51–60, 1994.
16. **Han Y, Runge MS, and Brasier AR.** Angiotensin II induces interleukin-6 transcription in vascular smooth muscle cells through pleiotropic activation of nuclear factor-κB transcription factors. *Circ Res* 84: 695–703, 1999.
17. **Keidar S.** Angiotensin, LDL peroxidation and atherosclerosis. *Life Sci* 63: 1–11, 1998.
18. **Keidar S, Kaplan M, and Aviram M.** Angiotensin II-modified LDL is taken up by macrophages via the scavenger receptor, leading to cellular cholesterol accumulation. *Arterioscler Thromb Vasc Biol* 16: 97–105, 1996.
19. **Ledebur HC and Parks TP.** Transcriptional regulation of the intercellular adhesion molecule-1 gene by inflammatory cytokines in human endothelial cells. Essential roles of a variant NF-κB site and p65 homodimers. *J Biol Chem* 270: 933–943, 1995.
20. **Li AC, Brown KK, Silvestre MJ, Willson TM, Palinski W, and Glass CK.** Peroxisome proliferator-activated receptor γ ligands inhibit development of atherosclerosis in LDL receptor-deficient mice. *J Clin Invest* 106: 523–531, 2000.
21. **Lin YL and Lin JK.** (−)-Epigallocatechin-3-gallate blocks the induction of nitric oxide synthase by down-regulating lipopolysaccharide-induced activity of transcription factor nuclear factor-κB. *Mol Pharmacol* 52: 465–472, 1997.
22. **Marx N, Sukhova GK, Collins T, Libby P, and Plutzky J.** PPARα activators inhibit cytokine-induced vascular cell adhesion molecule-1 expression in human endothelial cells. *Circulation* 99: 3125–3131, 1999.
23. **Moore KJ, Rosen ED, Fitzgerald ML, Randow F, Andersson LP, Altshuler D, Milstone DS, Mortensen RM, Spiegelman BM, and Freeman MW.** The role of PPAR-γ in macrophage differentiation and cholesterol uptake. *Nat Med* 7: 41–47, 2001.
24. **Nagy L, Tontonoz P, Alvarez JG, Chen H, and Evans RM.** Oxidized LDL regulates macrophage gene expression through ligand activation of PPARγ. *Cell* 93: 229–240, 1998.
25. **Newton R, Kuitert LM, Bergmann M, Adcock IM, and Barnes PJ.** Evidence for involvement of NF-κB in the transcriptional control of COX-2 gene expression by IL-1β. *Biochem Biophys Res Commun* 237: 28–32, 1997.
26. **Read MA, Whitley MZ, Williams AJ, and Collins T.** NF-κB and IκBα: an inducible regulatory system in endothelial activation. *J Exp Med* 179: 503–512, 1994.
27. **Ricote M, Huang J, Fajas L, Li A, Welch J, Najib J, Witztum JL, Auwerx J, Palinski W, and Glass CK.** Expression of the peroxisome proliferator-activated receptor γ (PPARγ) in human atherosclerosis and regulation in macrophages by colony stimulating factors and oxidized low density lipoprotein. *Proc Natl Acad Sci USA* 95: 7614–7619, 1998.
28. **Ridker PM, Hennekens CH, Roitman-Johnson B, Stampfer MJ, and Allen J.** Plasma concentration of soluble intercellular adhesion molecule 1 and risks of future myocardial infarction in apparently healthy men. *Lancet* 351: 88–92, 1998.
29. **Ross R.** The pathogenesis of atherosclerosis: an update. *N Engl J Med* 314: 488–500, 1986.
30. **Ross R.** Atherosclerosis is an inflammatory disease. *Am Heart J* 138: S419–S420, 1999.
31. **Rossi A, Kapahi P, Natoli G, Takahashi T, Chen Y, Karin M, and Santoro MG.** Anti-inflammatory cyclopentenone prostaglandins are direct inhibitors of IκB kinase. *Nature* 403: 103–108, 2000.
32. **Ruiz-Ortega M, Lorenzo B, Ruperez M, Blanco J, and Egido J.** Systemic infusion of angiotensin II into normal rats activates nuclear factor-κB and AP-1 in the kidney: role of AT(1) and AT(2) receptors. *Am J Pathol* 158: 1743–1756, 2001.
33. **Satta J.** Expansion and rupture of abdominal aortic aneurysms. *Ann Chir Gynaecol* 87: 63, 1998.
34. **Shu HB, Agranoff AB, Nabel EG, Leung K, Duckett CS, Neish AS, Collins T, and Nabel GJ.** Differential regulation of vascular cell adhesion molecule 1 gene expression by specific NF-κB subunits in endothelial and epithelial cells. *Mol Cell Biol* 13: 6283–6289, 1993.
35. **Siebenlist U, Franzoso G, and Brown K.** Structure, regulation and function of NF-κB. *Annu Rev Cell Biol* 10: 405–455, 1994.
36. **Staels B, Koenig W, Habib A, Merval R, Lebret M, Torra IP, Delerive P, Fadel A, Chinetti G, Fruchart JC, Najib J, Maclouf J, and Tedgui A.** Activation of human aortic smooth-

muscle cells is inhibited by PPARα but not by PPARγ activators. *Nature* 393: 790–793, 1998.

37. **Wang YX, Martin-McNulty B, Freay AD, Sukovich DA, Halks-Miller M, Li WW, Vergona R, Sullivan ME, Morser J, Dole WP, and Deng GG.** Angiotensin II increases urokinase-type plasminogen activator expression and induces aneurysm in the abdominal aorta of apolipoprotein E-deficient mice. *Am J Pathol* 159: 1455–1464, 2001.
38. **Weiss D, Sorescu D, and Taylor WR.** Angiotensin II and atherosclerosis. *Am J Cardiol* 87: 25C–32C, 2001.